

## Kinetics of chemical leaching of chalcocite from low-grade copper ore: size-distribution behavior

H. Naderi<sup>1</sup>, M. Abdollahy<sup>2\*</sup> and N. Mostoufi<sup>3</sup>

1. Department of Mining and Metallurgical Engineering, Yazd University, Yazd, Iran

2. Mining Engineering Department, Faculty of Engineering, Tarbiat Modares University, Tehran, Iran

3. School of Chemical Engineering, College of Engineering, University of Tehran, Tehran, Iran

Received 30 August 2014; received in revised form 26 January 2015; accepted 3 February 2015

\*Corresponding author: minmabd@modares.ac.ir (M. Abdollahy).

### Abstract

Kinetics of the chemical leaching of chalcocite from a low-grade copper ore in a ferric sulfate medium was investigated using the constrained least square optimization technique. The experiments were carried out for different particle sizes in both the reactor and column at constant Eh, pH, and temperature. The leaching rate increased with increase in the temperature. About 50% of the Cu recovery was obtained after 2 hours of reactor leaching at 75 °C using the -0.5 mm size fraction. Also about 50% of the Cu recovery was obtained after 60 days of column leaching for the +4-8 mm size fraction. For the fine-particle leaching, the first leaching step was fast, and the rate controlling step was diffusion through the liquid film. The results obtained show that as the leaching proceeds, the chemical reaction control appears. Finally, accumulation of the elemental sulfur layer in the solid product together with the jarosite precipitate causes change in the controlling mechanism to solid diffusion. For the coarse-particle leaching, diffusion through the solid product appeared from the initial days of leaching.

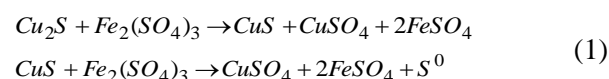
**Keywords:** *Leaching, Chalcocite, Kinetic Study, Shrinking Core Model (SCM).*

### 1. Introduction

Bacterially-assisted heap-leaching of low-grade copper sulfides is a developing technology that has been applied successfully to the extraction of copper from the secondary sulfide minerals such as chalcocite at a number of operations worldwide. However, heap-bioleaching of the refractory primary copper sulfide, chalcopyrite, is yet to be implemented at the commercial scale [1]. Currently, Mintek Company (South Africa) and National Iranian Copper Industries Company (NICICO) are undertaking a large-scale pilot test for the Mintek's heap-bioleaching technology for Darehzar copper ore at Sarcheshmeh Copper Complex located in the south of Iran. As a sub-process in heap-bioleaching, the chemical leaching of chalcocite from supergen ore was studied in this work. Kinetics of the chemical leaching of chalcocite from low-grade copper ore was investigated for different particle sizes. The experimental data was used to determine the

different rate-controlling steps at various leaching times by means of the constrained least square optimization technique.

Sullivan [2] has published the first detailed view of the chalcocite dissolution in an acid oxidation medium using ferric sulfate. He has found that chalcocite dissolves in two stages, according to the following reactions:



Stage I is considerably faster than stage II, and the former is almost completely independent from temperature, which indicates that the reaction is controlled by the mass transport. The second stage already depends greatly upon the temperature, and on the surface area of the dissolved particles. The experiments carried out have confirmed that if the amount of copper transferred into the solution is less than 50%, elemental sulfur does not form, and

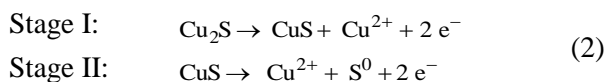
the solid phase CuS forms after the transfer of 50% of copper into the solution [2].

Two distinctive stages of the reaction have also been found by Warren [3] in the process of pressure-leaching of chalcocite in sulfuric acid. Stanczyk and Rampacek [4] have also observed two stages of the chalcocite solution in the process of pressure-leaching in sulfuric acid. Mulak [5] has confirmed the dissolution of chalcocite through the formation of the transitional product CuS. At the temperatures below 60 oC, the dissolution rate is controlled by the mass transport to the surface, with an activation energy of 6.3 kJ mol<sup>-1</sup>. At temperatures higher than 60 oC, the rate of the second stage of dissolution with the activation energy of 22 kJ mol<sup>-1</sup> is controlling.

King et al. [6] have investigated the kinetics of the dissolution of synthetic chalcocite by an acidified solution of ferric chloride. They have confirmed that the first, fast stage of the dissolution produces CuS, and it is followed by the second stage, in which the dissolution rate of this intermediate product is considerably low. The activation energy of the first stage of the dissolution reaction is 3.34 kJ mol<sup>-1</sup>, and it depended greatly upon the concentration of FeCl<sub>3</sub>. The activation energy of the second stage of dissolution is 101-122 kJ mol<sup>-1</sup>, and this has been interpreted as the chemically-controlled reaction.

The transformation of chalcocite to covellite has been investigated by X-ray diffractometry and electron microscopy. The results obtained have shown that the new sulfides formed change continuously, and the existence of the non-stoichiometric copper sulfides has been confirmed [6]. The existence of the non-stoichiometric phases (Cu<sub>1.96</sub>S, Cu<sub>1.8</sub>S) between chalcocite and covellite has also been confirmed by the results obtained by Burkin [3].

Marcantonio [7] has expressed the two stages of the chalcocite dissolution with the following anodic half-cells:



According to Petersen et al. [8-9] and Bolorunduro [10], the first step involves the formation of a pseudo-covellite intermediate sulfide product (also known as blaubleibender), which is subsequently oxidized to the elemental sulfur. The rate of the first step is very rapid, and controlled by the solid-state diffusion of copper in the sulfide lattice and the mass transport of ferric ions to the mineral surface. Therefore, it exhibits a

low activation energy. The second step is much slower, controlled by the rate of charge transfer in the anodic decomposition process, and has an extremely high activation energy (80–100 kJ mol<sup>-1</sup>).

## 2. Experimental procedure

The copper ore used in this study was obtained from the enrichment zone of the Darehzar copper mine (Kerman, Iran). The ore was crushed 100% <2.5 cm using a jaw crusher, and was split into multiple-size fractions. Each size fraction was mixed and split to produce the representative sample charges. Chemical analyses were carried out using atomic absorption spectroscopy (AAS), Perkin-Elmer 2100. Mineralogical analyses of the samples were performed by X-ray diffraction (XRD) (Philips PW 1730, Co-K $\alpha$  accelerating voltage 30mA–40kV). Scanning electron microscopy (SEM) and energy dispersive X-ray spectroscopy (EDAX) analyses of the particle surfaces were carried out using Philips (XL30).

All the tests were performed at constant pH and Eh, which were adjusted to the initial values with NaOH or H<sub>2</sub>SO<sub>4</sub> and H<sub>2</sub>O<sub>2</sub> solutions. Leaching of the -0.5 mm size fraction was performed in a 1.5-L glass vessel equipped with a water jacket, an overhead reflux condenser, a stirring shaft, and an overhead variable speed stirrer at a pulp density of 35 g L<sup>-1</sup>. Three tests were carried out at 55, 65, and 75 °C, while the other parameters were kept constant. Leaching of the coarse-size fractions (+4 -8 mm, +8 -12.7 mm, +12.7 -25 mm) was done in a 50-cm long column (7 cm in diameter), loaded with 2 kg of the representative ore. The column was operated in the solution-recycle mode for one week using a dilute solution of H<sub>2</sub>SO<sub>4</sub> (pH 1.8) in order to dissolve the acid-soluble ore components. Then the column was heated to 70°C, and the reservoir solution was maintained at pH 1.4 by adding concentrated H<sub>2</sub>SO<sub>4</sub>, as required, for the duration of the experiment. The column was irrigated up-flow at a rate of 1 L min<sup>-1</sup> by a 0.5 g L<sup>-1</sup> of Fe solution (Fe<sup>+3</sup>/Fe<sup>+2</sup>=0.2, resulting in the initial ferric ion concentration of 0.08 g L<sup>-1</sup>) in order to obtain Eh=400 mV (Pt-Ag/AgCl). This solution was re-circulated continuously throughout the test.

## 3. Kinetic modeling

Chalcocite dissolution consists of two stages. During the first stage, chalcocite is transformed into covellite. If the reaction proceeds topo-chemically, a layer of covellite will form over a chalcocite core, which will shrink until the

conversion into covellite is completed. Therefore, the shrinking core model (SCM) for the spherical particles of unchanging size can be used to describe the kinetics of the chalcocite leaching. SCM consists of the following main steps:

Step 1: Diffusion of the leachant through the liquid film surrounding the particle.

Step 2: Diffusion of the leachant through the product layer at the surface of the unreacted core.

Step 3: Chemical reaction of the leachant at the surface of the core with the reactant.

In order to determine the mechanism of leaching, the formula of each controlling step was tested against the experimental data, and the mechanism that best fitted the experimental data was chosen as the controlling step.

Nazemi et al. [11] have proposed a procedure in which all of the above three steps can be taken into account in determining the kinetics of leaching by SCM. In this approach, for finding the controlling steps in the leaching process, the simultaneous actions of these steps, which act in series, are combined together as follow [12]:

$$t = \tau_F X + \tau_P \left( 1 - 3(1-X)^{2/3} + 2(1-X) \right) + \tau_R \left( 1 - (1-X)^{1/3} \right) \quad (3)$$

where,

$$\tau_F = \frac{\rho_s R_0}{3bk_l C_{Ab}} \quad (4)$$

$$\tau_P = \frac{\rho_s R_0^2}{6bD_e C_{Ab}} \quad (5)$$

$$\tau_R = \frac{\rho_s R_0}{bk_s C_{Ab}} \quad (6)$$

Contribution of each of the above-mentioned steps in the kinetics of leaching can be revealed by fitting the experimental data to Equation (3), and evaluating the constants  $\tau_F$ ,  $\tau_P$ , and  $\tau_R$  in the equation. These constants are calculated by a multi-linear regression analysis using the least square technique. However, an unconstrained least square optimization may result in negative values for one or more constants, which are physically unacceptable based upon their definitions. To overcome this difficulty, Nazemi et al. [11] have proposed a constrained least square technique to determine the constants in Equation (3), as follows:

$$\varphi = \sum_i \left[ \tau_F X_i + \tau_P \left( 1 - 3(1-X_i)^{2/3} + 2(1-X_i) \right) + \tau_R \left( 1 - (1-X_i)^{1/3} \right) - t_i \right]^2 \quad (7)$$

$$\text{Min} \varphi \quad (8)$$

subject to  $\tau_F$ ,  $\tau_P$ , and  $\tau_R > 0$ .

Equation (8) is an optimization problem, which can be solved by any optimization technique to evaluate  $\tau_F$ ,  $\tau_P$ , and  $\tau_R$ . This approach has the advantage of revealing the controlling steps in a single-stage calculation. In addition, it is capable of identifying the possibility of the existence of mixed mechanisms, which cannot be determined easily using the conventional methods.

If there are two leaching stages (i.e. the trend of leaching changes at a specific time after the start of the leaching process), Equation (8) cannot be directly applied to the second stage, since the boundary condition for this stage is different from that of Equation (8) (zero recovery at  $t = 0$ ). Arabi et al. [13] have proposed the same type of data-processing for the second stage of leaching using the following generalized formula instead of Equation (3):

$$t - t_1 = \tau_F (X - X_1) + \tau_P \left[ 1 - 3 \left( \frac{1-X}{1-X_1} \right)^{2/3} + 2 \left( 1 - (1-X_1)^{1/3} (X - X_1) \right) \right] + \tau_R \left[ 1 - \left( \frac{1-X}{1-X_1} \right)^{1/3} \right] \quad (9)$$

where,

$$\tau_F = \frac{\rho_s R_0 (1 - X_1)^{1/3}}{3bk_l C_{Ab}} \quad (10)$$

$$\tau_P = \frac{\rho_s R_0^2 (1 - X_1)^{2/3}}{6bD_e C_{Ab}} \quad (11)$$

$$\tau_R = \frac{\rho_s R_0 (1 - X_1)^{1/3}}{bk_s C_{Ab}} \quad (12)$$

In this case, the objective function, from which the constants are obtained, would be as follows:

$$\varphi = \tau_F (X - X_1) + \tau_P \left[ 1 - 3 \left( \frac{1-X}{1-X_1} \right)^{2/3} + 2 \left( 1 - (1-X_1)^{1/3} (X - X_1) \right) \right] + \tau_R \left[ 1 - \left( \frac{1-X}{1-X_1} \right)^{1/3} \right] - (t - t_1) \quad (13)$$

## 4. Results and discussion

### 4.1. Ore mineralogy

According to the XRD analysis, the Darehzar copper ore mainly consists of silicate matrix. The major minerals identified included quartz, mica, clay minerals, and feldspar. The mineralogical analysis performed showed that the main copper mineral was chalcopyrite, which was altered into chalcocite (Figure 1).



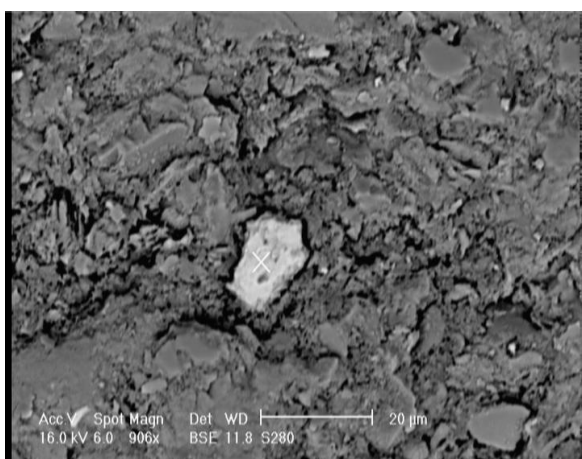
Figure 1. Alteration of chalcopyrite into chalcocite.

Table 1. Chemical analysis of different-sized fractions of enrichment zone ore (weight %).

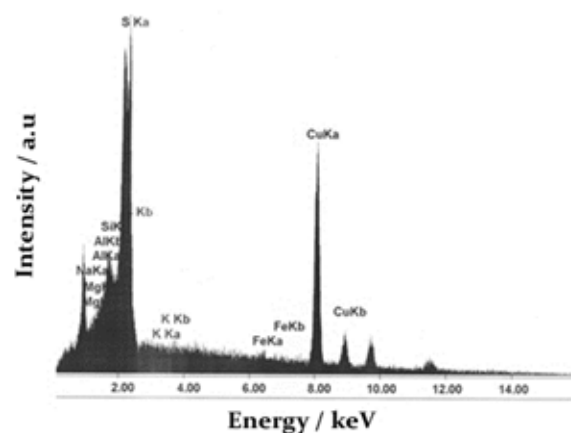
Size	Elements								
	Cu	Fe	S	SiO <sub>2</sub>	Al <sub>2</sub> O <sub>3</sub>	Mo	FeO	CuO	Others
-0.5 mm	0.37	7.97	8.37	49.92	17.85	0.010	0.72	0.10	14.710
+4-8 mm	0.25	4.23	3.92	59.19	17.82	0.004	0.54	0.06	13.996
+8-12.7 mm	0.23	4.49	3.92	57.04	17.61	0.007	0.40	0.06	16.253
+12.7-25 mm	0.23	3.70	3.06	60.15	17.82	0.004	0.68	0.05	14.316

Table 1 shows the chemical analysis of different-sized fractions. According to the results obtained, the maximum amount of (possible) chalcocite or chalcopyrite is less than 0.5%, which falls in the detection limits of the conventional XRD. Therefore, SEM-EDAX was used to detect copper minerals (Figure 2). The variations in the mineralogical composition of the particle sizes show that the Cu content increases with reduction in the particle size.

Table 2 illustrates the mineralogical analysis of each size fraction, and Table 3 shows the copper contribution related to different phases. As illustrated, about 16-19% of the copper content is in the oxide phase, and less than 30% of it is in the chalcopyrite phase. The particle size of +12.7-25 mm has the least pyrite content, while the particle size of -0.5 mm has the highest pyrite content.



(a)



(b)

Figure 2. SEM (a) and EDAX (b) analyses of copper mineral in ore.

**Table 2. Mineralogical analysis of different-sized fractions of enrichment zone ore (concentration %).**

Size	Chalcocite	Covellite	Chalcopyrite	Pyrite
-0.5 mm	0.212	0.085	0.156	16.51
+4-8 mm	0.146	0.026	0.190	8.66
+8-12.7 mm	0.072	0.124	0.116	8.66
+12.7-25 mm	0.131	0.046	0.145	7.61

**Table 3. Cu% at different phases.**

Size	Chalcocite	Covellite	Chalcopyrite	CuO
-0.5 mm	49.14	16.50	15.82	18.54
+4-8 mm	48.52	7.24	27.63	16.62
+8-12.7 mm	26.00	37.54	18.35	18.11
+12.7-25 mm	46.60	13.69	22.60	17.11

#### 4.2. Effect of temperature

The effect of temperature on the leaching of Cu from the -0.5 mm size fraction is shown in Figure 3. The copper oxide phase leached almost immediately, and was subtracted from the total copper leached. As illustrated, the rate of leaching increased with increase in the temperature, and more than 50% of Cu was extracted at 75°C after 2 h.

The effect of temperature on the first stage of the dissolution rate is consistently little in the first stage of chalcocite leaching, and that reaction proceeds rapidly at room temperature. The

kinetics of the second stage of the dissolution rate is much slower and more temperature-sensitive than that of the first stage. The reaction rate is extremely slow at room temperature, and increases with increase in the temperature.

According to Table 2, about 50% of the total Cu content (60% of the Cu content in the sulfide phase) is in the chalcocite phase. Usually, about 40% of Cu from the chalcocite phase dissolves at the first stage of leaching [5,14]. This is equal to 24% of the Cu content in the sulfide phase, dissolved before 30 min at all temperatures.

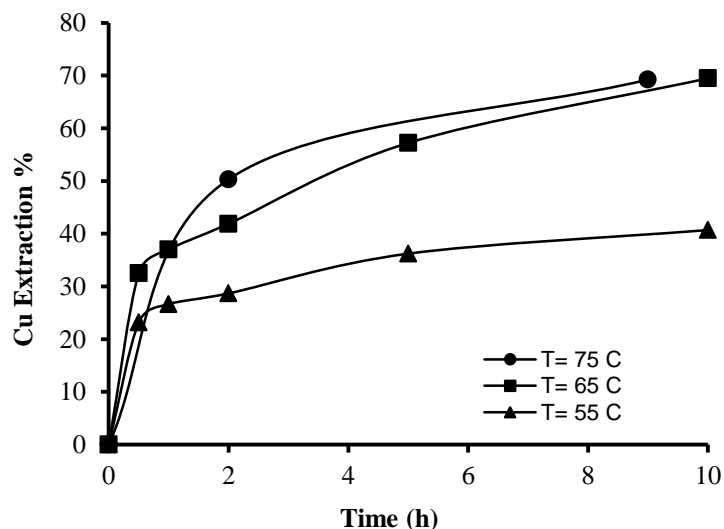


**Figure 3. Effect of temperature on chemical leaching of Cu from enrichment zone ore (sulfide phase; copper oxide phase is subtracted from total copper leached); (-0.5 mm size fraction,  $E_h=400$  mV (vs. Ag/AgCl), pH=1.4,  $Fe_{total}=0.5$  g L<sup>-1</sup>).**

#### 4.3. Kinetics

Figure 4 shows the Cu extraction results obtained from the column leaching tests. Figures 3 and 4 suggest that the mechanism for the short-time leaching is different from that for the long-time leaching, since the slopes for the curves at these periods are noticeably different. In order to check this, the formula for the chemical reaction control was tested against the experimental data

of -0.5mm size fraction at 55oC, as shown in Figure 5.

According to this figure, the leaching trend changes during the experiment, confirming that there are at least two stages in the leaching of chalcocite ores. The same trend was observed for the column-leaching experiments.

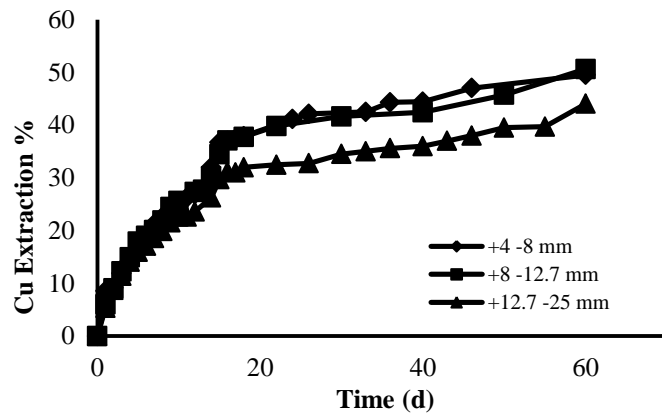


Figure 4. Rate of copper extraction via column-leaching for different size fractions. Temperature=70 °C,  $E_h=400$  mV (vs. Ag/AgCl), pH=1.4,  $Fe_{total}=0.5$  g L<sup>-1</sup>.

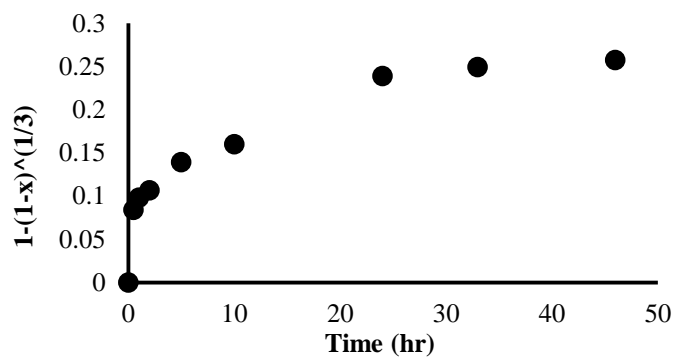


Figure 5. Fitting shrinking core equation of chemical control to leaching data of -0.5 mm size fraction at 55 °C.

#### 4.3.1. Leaching of -0.5 mm size fraction

The data shown in Figure 3 were used to investigate the kinetics of the leaching of -0.5mm size fraction at 55°C in the reactor. Different time intervals were considered for investigating the leaching mechanism at the different leaching stages. The results obtained for fitting the experimental data to Equations (8) and (13) by the constrained least square technique are shown in Table 4.

It can be concluded from Table 4 that the first leaching step is fast, and the rate-controlling step is diffusion through the liquid film. Since the particle size is small, it can be expected that the liquid film surrounding the particles provides high resistance against the mass transfer, confirmed by the data analysis in this section.

In a review paper on ferric leaching of sulfides, Dutrizac and Macdonald [15] have tabulated the findings of all the previous kinetic studies on chalcocite and covellite. According to their findings, the first stage of chalcocite leaching is very fast, relative to its second stage or to the leaching of natural covellite. The rate of the first stage is controlled by the diffusion of oxidant to the mineral surface. This view is supported by the observed low activation energies. The activation

energy of 17 kJ mol<sup>-1</sup> was determined for the first stage of chalcocite leaching. This value falls in the range expected for the rate limited by the boundary layer diffusion.

At the second stage, the newly formed covellite and the covellite initially present in the ore react, and the chemical reaction control becomes the rate-limiting mechanism.

During the second stage of leaching, covellite reacts, leaving a shell of sulfur surrounding a shrinking core of unreacted covellite. Since the sulfur layer is not capable of electronic conduction, the oxidant should diffuse toward the shrinking core of the unreacted CuS. Consequently, diffusion of the oxidant species through the growing layer of sulfur becomes the rate-limiting process at this stage [14]. At the same time, absence of iron control allows the spontaneous formation of jarosite, which may coat the remaining covellite, and decrease the rate of dissolution due to the mass transport and/or reduced surface area (Figure 6). As it could be seen in Table 3, after 5 h, diffusion through the product layer becomes the rate-controlling process.

The activation energy of  $140\text{kJ mol}^{-1}$  was determined for the second stage of chalcocite leaching, confirming the above-mentioned results. Figure 6 shows the SEM-EDAX analysis result

for particle surfaces after leaching. Sulfur-and iron-bearing compounds can be seen clearly on the particle surfaces.

**Table 4. Evaluated constants for leaching of -0.5 mm size fraction at 55 °C.**

Time interval, h	$\tau_F$	$\tau_P$	$\tau_R$	Correlation coefficient, $r^2$
0-0.5	1.37	0	0	0.9999
0.5-5	0	0	141.57	0.9999
5-10	0	618.70	0	0.9645

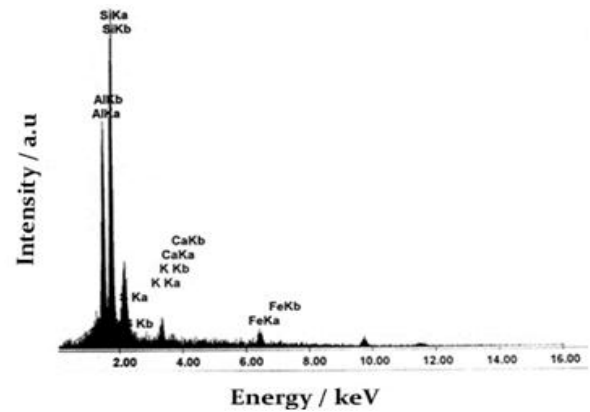
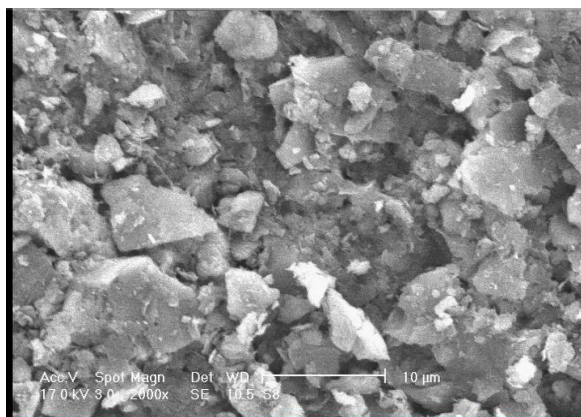


**Figure 6. SEM (a) and EDAX (b) analyses of particle surfaces after leaching, -0.5 mm size fraction.**

**4.3.2. Leaching of coarse particles**

The data shown in Figure 4 was used to investigate the kinetics of the column-leaching of different size fractions. The results obtained for fitting the experimental data to Equations (8) and (11) by the constrained least square technique are shown in Tables 5-7.

During the first week of +4-8 mm size fraction leaching, the chemical reaction control and diffusion through the product layer were the rate-controlling steps (Table 5). During the initial leaching phase, the small mineral grains exposed at the surface leached relatively rapidly. Subsequently, additional mineral surfaces were required to be exposed, either by dissolution of gangue or penetration of the leaching solution into the mineral grains. As the leaching proceeds, diffusion through the product layer is the only

rate-limiting mechanism. Jarosite and other precipitated ferric sulfates are usually produced during the heap-leaching of low-grade ores with ferric sulfate (Figures 8 and 9). This phenomenon involves an additional important barrier. Figure 7 shows the variation in Fe concentration in the leaching solution during the column-leaching experiments. Decrease in the Fe concentration after the 30th day shows iron precipitation. Figure 8 shows the SEM-EDAX analysis of the particle surfaces after leaching. Sulfur-and iron-bearing compounds can be clearly seen on the particle surfaces.

According to Table 6, during the first 4 days of +8-12.7 mm size fraction leaching, combination of the chemical reaction and diffusion through the product layer is the rate-controlling mechanism.

**Table 5. Evaluated constants for column-leaching of +4 -8 mm size fraction.**

Time interval/d	$\tau_F$	$\tau_P$	$\tau_R$	Correlation coefficient, $r^2$
1-7	0	142.54	98.43	0.9992
12-30	0	$1 \times 10^3$	0	0.9174

**Table 6. Evaluated constants for column-leaching of +8 -12.7 mm size fraction.**

Time interval/d	$\tau_F$	$\tau_P$	$\tau_R$	Correlation coefficient, $r^2$
1-4	0	263.00	18.15	0.9999
5-13	0	770.19	83.68	0.9780
16-26	0	$1.49 \times 10^3$	0	0.9731

**Table 7. Evaluated constants for column-leaching of +12.7 -25 mm size fraction.**

Time interval/d	$\tau_F$	$\tau_P$	$\tau_R$	Correlation coefficient, $r^2$
1-3	0	0.001	107.93	0.9999
6-12	0	$1.37 \times 10^3$	30.90	0.9829
14-28	0	$5.45 \times 10^3$	0	0.9772

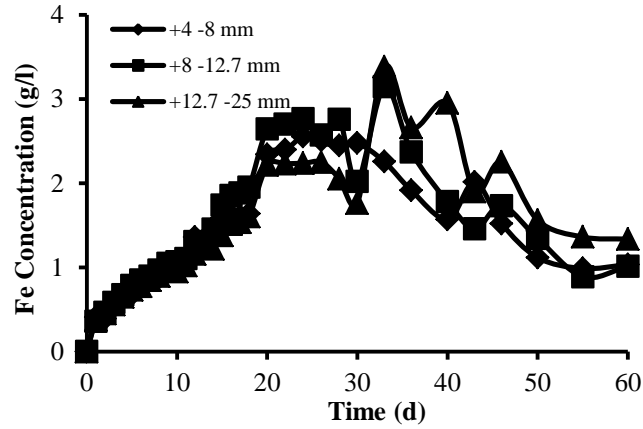
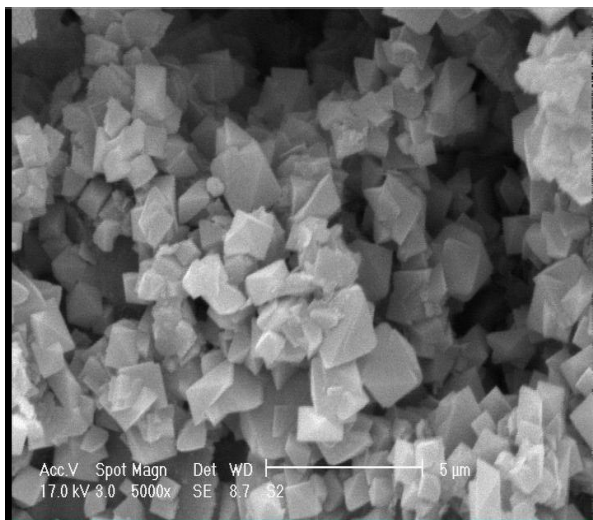
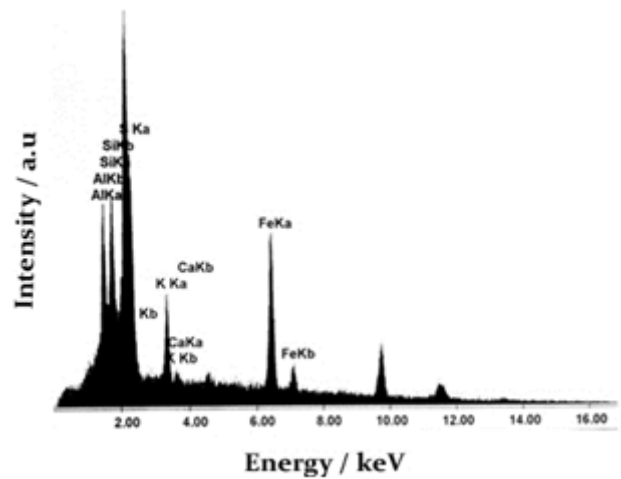


**Figure 7. Variation in Fe concentration in leaching solution during column-leaching experiments.**

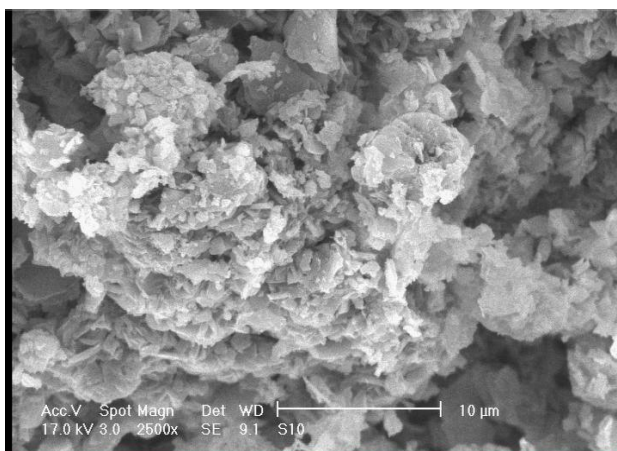


(a)

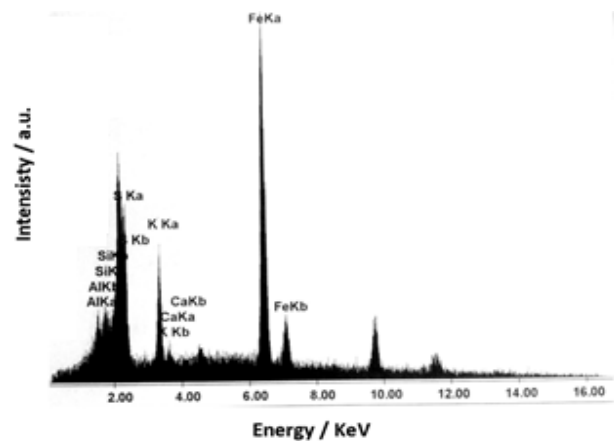


(b)

**Figure 8. SEM (a) and EDAX (b) analyses of the particle surfaces after column leaching, +4 -8 mm size fraction.**



(a)



(b)

**Figure 9. SEM (a) and EDAX (b) analyses of particle surfaces after column leaching, +12.7 -25 mm size fraction.**

Particle breakage during the first stage enhances the dissolution of the second stage covellite by providing fresh and large surfaces for chemical reaction [10]. Therefore, the same steps were observed as the rate-controlling mechanisms again. Accumulation of the elemental sulfur layer in the solid product accompanied with jarosite precipitate, changes the controlling mechanism into solid diffusion.

A similar trend was observed for the +12.7-25 mm size fraction (Table 7). However, the coefficient for the solid diffusion mechanism was higher, compared to the +8 -12.7 mm size fraction. Figure 9 shows the SEM-EDAX analysis of particle surfaces after leaching. Sulfur-and iron-bearing compounds can be clearly seen on the particle surfaces.

## 5. Conclusions

Copper leaching from low-grade ore-containing chalcocite and covellite in ferric sulfate media, and its kinetic aspects for different particle size fractions, including fine and coarse particles, were studied using a statistical approach. The experiments were carried out for different particle sizes in both a reactor and a column at constant Eh, pH, and temperature. The leaching rate increased with increase in the temperature. At 75 °C, more than 50% of Cu was extracted after 2 h. The kinetic investigation revealed that for the fine particles, the first leaching step was fast, and the rate-controlling step was diffusion through the liquid film. During the second leaching stage, covellite reacted, leaving a shell of sulfur surrounding a shrinking core of unreacted covellite, and chemical reaction controlled appeared. Finally, accumulation of the elemental sulfur layer in the solid product, accompanied with jarosite precipitate, changed the controlling mechanism into solid diffusion. For the leaching of coarse particles, diffusion through the solid product appeared from the initial days of leaching.

## Nomenclature

$b$	stoichiometric coefficient
$c$	concentration of sulfuric acid ( $\text{kg m}^{-3}$ )
$d$	characteristic length (particle diameter) (m)
$D$	molecular diffusion coefficient ( $\text{m}^2 \text{s}^{-1}$ )
$D_e$	effective diffusion coefficient in porous structures $\text{m}^3 \text{fluid/m solid.s}$ )
$k_s$	reaction rate constant ( $\text{s}^{-1}$ )
$R_0$	initial radius of particle (m)
$R$	radius of reference size class, mean radius (m)

$r^2$	correlation coefficient
$t$	time of reaction (s)
$t_1$	start of long time period (s)
$X$	fraction of reacted chalcocite
$X_1$	fraction of reacted chalcocite at time $t_1$

## Greek symbols

$\rho$	density ( $\text{kg m}^{-3}$ )
$\tau$	time for complete conversion of a reactant particle to product (s)

## Acknowledgements

The authors gratefully acknowledge the support of Research & Development Division of Sarcheshmeh Copper Complex (Kerman, Iran) and Tarbiat Modares University (Tehran, Iran).

## References

- [1]. Watling, H. R. (2006). The bioleaching of sulfide minerals with emphasis on copper sulphides- A review. *Hydrometallurgy*. 84: 81-108.
- [2]. Sullivan, J. D. (1933). Chemical and physical features of copper leaching. *Trans. Am. Inst. Min. Metall.* 106: 515-546.
- [3]. Havlik, T. (2008). *Hydrometallurgy: Principles and Applications*. Cambridge International Science Publishing Limited, 388 p.
- [4]. Stanczyk, M. H. and Rampacek, C. (1963). Oxidation leaching of copper sulfides in acidic pulps at elevated temperatures and pressures. [Washington, D. C.]: Bureau of Mines.
- [5]. Mulak, W., Kinetics of cuprous sulfide dissolution in acidic solutions of ferric sulfate, *Rocz. Chem.*, 43: 1387-1969.
- [6]. King, J. A., Burkin, A. R. and Ferreira, R. C. H. (1975). Leaching of chalcocite by acidic ferric chloride solutions. *Leaching and Reduction in Hydrometallurgy*. IMM London. 36-46.
- [7]. Marcantonio, P. (1975). Kinetics of dissolution of chalcocite in ferric sulfate solutions, Ph.D. thesis, Dep. of Mining, Metallurgical and Fuels Engineering, University of Utah, Lake Utah, USA.
- [8]. Petersen, J. and Dixon, D. G. (2007). Principles, mechanisms and dynamics of chalcocite heap bioleaching, *Microbial Processing of Metal Sulfides*, Springer Netherlands, pp. 193-218.
- [9]. Petersen, J. and Dixon, D. G. (2007). Modelling and optimization of heap bioleach processes, *Biomining*, Springer Berlin Heidelberg, pp. 153-176.
- [10]. Bolorunduro, S. A. (1999). Kinetics of leaching of chalcocite in acid ferric sulfate media: Chemical and bacterial leaching, MSc thesis, Dep. of Metals and Materials Engineering, University of British Columbia.

[11]. Nazemi, M. K., Rashchi, F. and Mostoufi, N. (2011). A new approach for identifying the rate controlling step applied to the leaching of nickel from spent catalyst. *International Journal of Mineral Processing*. 100 (1-2): 21-26.

[12]. Levenspiel, O. (1999). *Chemical Reaction Engineering*. Second ed. John Wiley and Sons, New York, USA.

[13]. Aarabi-Karasgani, M., Rashchi, F., Mostoufi, N. and Vahidi, E. (2010). Leaching of vanadium from LD

converter slag using sulfuric acid. *Hydrometallurgy*. 102 (1-4): 14-21.

[14]. Ruiz, M. C., Honores, S. and Padilla, R. (1998). Leaching kinetics of degenite concentrate in oxygenated chloride media at ambient pressure. *Metallurgical and Materials Transactions B*. 29B: 961-969.

[15]. Dutrizac, J. E. and MacDonald, R. J. C. (1974). Ferric ion as a leaching medium. *Minerals Science and Engineering*. 6 (2): 59-100.

## مطالعه سینتیک لیچینگ شیمیایی کالکوسیت از کانه کم‌عیار مس: رفتار بخش‌های مختلف ابعادی

حجت نادری<sup>۱</sup>، محمود عبدالهیی<sup>۲\*</sup> و نوید مستوفی<sup>۳</sup>

۱- دانشکده معدن و متالورژی، دانشگاه یزد، ایران

۲- بخش معدن، دانشکده فنی و مهندسی، دانشگاه تربیت مدرس، ایران

۳- دانشکده مهندسی شیمی، پردیس فنی و مهندسی، دانشگاه تهران، ایران

ارسال ۲۰۱۴/۸/۳۰، پذیرش ۲۰۱۵/۲/۳

\* نویسنده مسئول مکاتبات: minmabd@modares.ac.ir

---

### چکیده:

در این تحقیق، سینتیک لیچینگ شیمیایی کالکوسیت از کانه کم‌عیار مس در محیط اسیدسولفوریک و در حضور یون فریک مطالعه شد. از روش کمترین مربعات خطا برای بهینه‌سازی استفاده شده است. آزمایش‌های لیچینگ بخش‌های مختلف ابعادی در رآکتور و ستون در شرایط ثابت Eh، pH و دما انجام شد. نتایج نشان داد که با افزایش دما، سرعت انحلال افزایش می‌یابد. در لیچینگ بخش ۵/۰- میلی‌متر در رآکتور در دمای ۷۵ درجه سانتی‌گراد، حدود ۵۰٪ از مس پس از دو ساعت حل شد. در لیچینگ ستونی بخش ابعادی ۸-۴ میلی‌متر، حدود ۵۰٪ از مس بعد از ۶۰ روز بازیابی شد. برای ذرات ریز، مرحله اول لیچینگ سریع بوده و نفوذ در لایه فیلم مایع کنترل‌کننده فرآیند انحلال است و با گذشت زمان کنترل شیمیایی ظاهر می‌شود. در نهایت تجمع گوگرد عنصری در سطح ذرات و تشکیل رسوب ژاروسیت، سبب می‌شود تا کنترل در لایه خاکستر ظاهر شود. در مورد لیچینگ ذرات درشت، نفوذ در لایه خاکستر از همان روزهای ابتدایی فرآیند به‌عنوان کنترل‌کننده واکنش انحلال ظاهر می‌شود.

**کلمات کلیدی:** لیچینگ، کالکوسیت، مطالعه سینتیک، مدل هسته انقباضی.

---